



## Impact of climate change on seawater intrusion, and shore line advance in Nile Delta, Egypt

Mohamed S. Taha <sup>1</sup>, Asaad M. Armanuos <sup>2</sup>, Bakenaz A. Zeidan <sup>3</sup>

<sup>1</sup> Demonstrator, Faculty of Engineering, Delta University, Gamsa, Egypt. MSc. Student, Faculty of Engineering, Tanta University.

<sup>2</sup> Associate Professor, Department of Irrigation and Hydraulic Engineering, Faculty of Engineering, Tanta University, Egypt.

<sup>3</sup> Professor of water resources, Faculty of Engineering, Tanta University, Egypt.

### ABSTRACT

Climate change is one of the most significant issues facing humanity, and an increased number of countries are proactively addressing this problem. Any changes in water resources brought on by climate change would pose a serious risk to a lot of nations. Egypt is one of these nations which will suffer from climate change. One of the consequences of climate change is sea level rise (SLR), which in turn will lead to the advance of shore line in land and more seawater intrusion. The sea water will advance inland, flooding a significant portion of the good lands, and many inhabitants will leave their homes as a result. The Nile Delta is one of the most vulnerable areas to be inundated by sea water due to the flat topographical nature of the area. Moreover, a large part of the water in the Nile Delta aquifer (NDA) will become saline, and the reservoir will become more vulnerable to Seawater intrusion (SWI) Which is affected not only by the rise in sea level and the advance of shore line, but also by the excessive withdrawal from the pumping wells .In this paper (MODFLOW+SEAWAT+ARC GIS) were used to investigate seawater intrusion in Nile Delta aquifer and to determine the position of the new shore line due to 0.25 m and 0.5 m rise of the Mediterranean sea level in Nile Delta. Owing to the lack of data of the topography of the area, because it need high accuracy of Digital Elevation Model (DEM) the position of shore line is obtained based on analyzing the results of saltwater intrusion due to 0.25 m and 0.5 m of sea level rise of recent studies through SEAWAT and the results were exported to ARC GIS to get maps of new shore line.

**Keywords:** Climate Change, Sea Level Rise, Nile Delta Aquifer, Seawater Intrusion, MODFLOW.

### 1. Introduction

Climate change is accelerating at a shocking rate as a result of human activities and natural processes. The majority of climatologists believe that human activities are mostly to blame for climate change because they increase greenhouse gas emissions, which raise earth's temperature. However, the vast majority of climatologists believe that the recent warming has only been somewhat influenced by tiny increases in solar energy. Significant ice from glaciers, ice sheets, and polar caps may melt as a result of long-term climate change. Because of this, sea levels would rise globally. Many coastal areas would face flooding, erosion, the loss of wetlands, and the incursion of seawater into fresh groundwater aquifers, as shown in (Figure 1). High flood levels would submerge certain coastal towns, little island nations, and other livable locations (Abd-Elhamid, 2010).

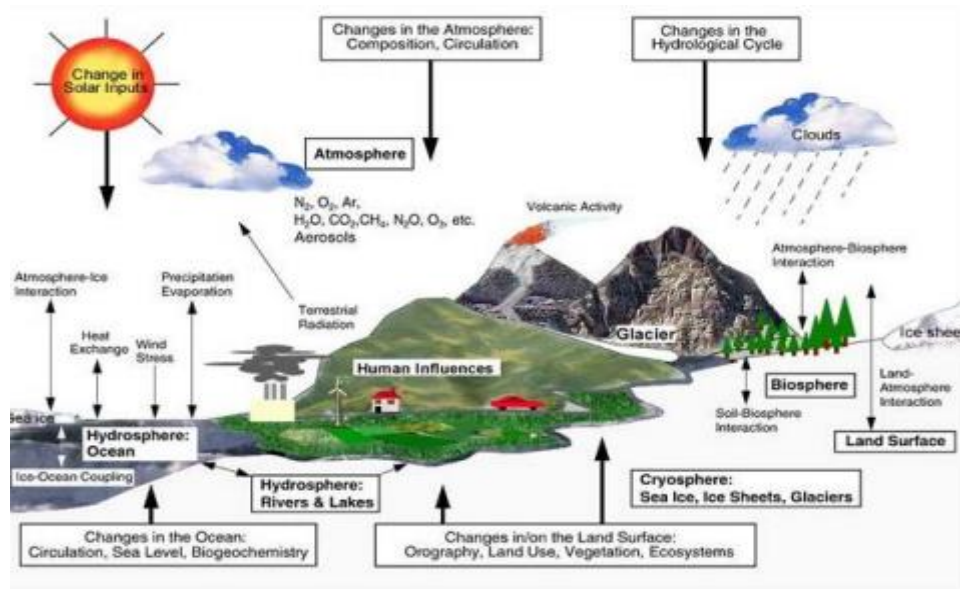


**Figure 1:** An illustration of the parts of the global climate system (Ismail, 2014)

A change in climate can result from both the climate system's inherent unpredictability and outside factors (both anthropogenic and natural). The influence of external sources on climate may be widely compared using the concept of radiative forcing. Typically, a positive radiative forcing—such as that caused by growing greenhouse gas concentrations—warms the surface. Some types of aerosols (microscopic airborne particles) can produce a negative radiative forcing that can cool the surface when they are present in greater quantities. Natural phenomena like unpredictable volcanic activity or fluctuations in solar output can also cause radiative forcing.

The amount of greenhouse gases in the entire atmosphere, which is mostly composed of nitrogen and oxygen, is less than 0.1%. Carbon dioxide is the most common greenhouse gas by far. Carbon dioxide (CO<sub>2</sub>), methane (CH<sub>4</sub>), nitrous oxide (N<sub>2</sub>O), sulphur hexafluoride (SF<sub>6</sub>), hydrofluorocarbons (HFCs), perfluorocarbons (PFCs), ozone-depleting chlorofluorocarbons (CFCs), and hydrochlorofluorocarbons are the greenhouse effect gases (HCFCs). (Figure 2) shows how human activity has increased the amount of greenhouse gases in the atmosphere, which appears to be disrupting the equilibrium between incoming and departing energy (IPCC, 2001)

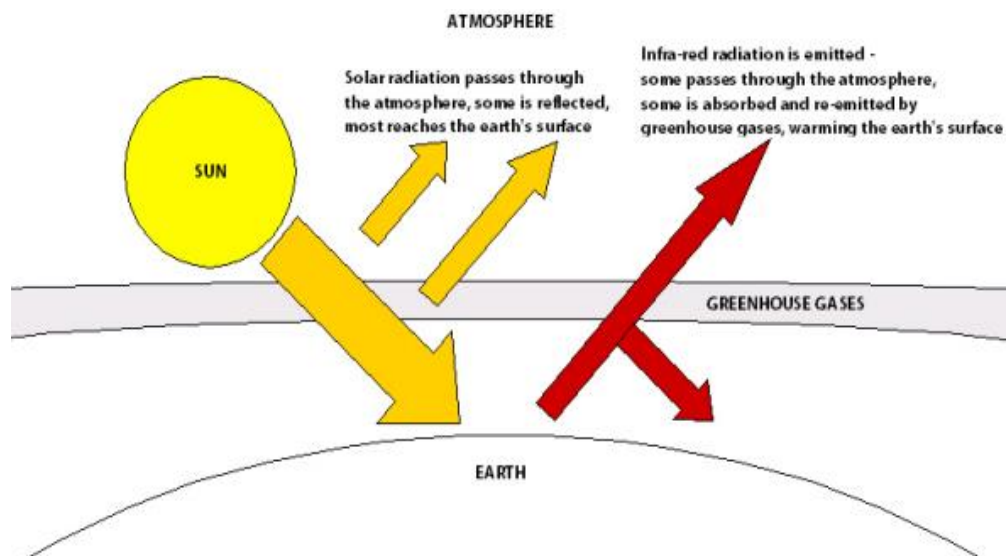


**Figure 2:** Greenhouse gas effect (Ismail, 2014)

Seawater intrusion and groundwater resource contamination are two indirect consequences on coastal areas that worsen soil salinity and endanger food security. According to a Met Office Hadley Centre (2011) assessment citing numerous studies, Egypt is highly vulnerable to sea level rise (SLR). Egypt was ranked as

the second most severely impacted country in terms of the shoreline population affected and the fifth highest in terms of the proportion of affected urban zones in one study that considered the impacts of a 1.0 m SLR for 84 developing countries.

As a result of subsidence, erosion, and accretion of the coastline, as well as sea level rise brought on by climate change, the Nile Delta region is currently changing. According to (Agrawala et al., 2004), the coastal zone of the Nile Delta is especially vulnerable to the effects of sea level rise because of direct inundation and saltwater intrusion. Low elevation coastal areas are regarded as high risk zones due to sea level rise (SLR). (El-Raey, 1994) assessed the vulnerability of Alexandria City to expected SLR, the SLR is anticipated to be between 0.5 and 1.0 metres in this century. The findings of the IPCC's fourth assessment report indicated that, based on the most likely scenario, a global SLR of 18 to 59 cm is projected by the end of this century, according to the 2nd Communication National Report (SNC, 2010). Using these numbers and accounting for the rates of land subsidence in the west, middle, and east delta, (CORI, 2008) determined the vulnerable areas that will be affected by sea level rise under two scenarios of lake boundaries. In the first instance, lake borders were deemed to have zero levels, while in the second, they were deemed to be protected. Three scenarios, including the IPCC scenarios B1 and A1FI as well as the new CoRI scenario, which assumes a linear rise in sea level until 2100, were considered for each model. Table 1 lists the areas of the Nile delta that are most vulnerable under the worst case scenario A1FI for the situation involving the boundaries of protected lakes. The bulk of lake borders are actually above zero (often between 0.50 m and 2.50 m).

**Table 1:** The situation of protected lake boundaries, the Nile Delta vulnerable zones, and the A1FI scenario

Year	2025			2050			2075			2100		
	W	M	E	W	M	E	W	M	E	W	M	E
SLR(cm)	13.00	14.80	27.90	34.00	37.50	68.80	55.00	60.30	109.60	72.00	79.00	144.00
Affected area km <sup>2</sup>	29.70	63.70	59.50	38.70	140.70	76.90	80.10	284.00	85.70	104.50	565.80	91.00
% of Nile Delta Area	0.12	0.25	0.24	0.16	0.56	0.31	0.32	1.14	0.34	0.42	2.26	0.36
Total affected area km <sup>2</sup>	152.85			256.29			449.80			761.30		
% of Nile Delta Area	0.61			1.03			1.80			3.04		

W: West of Delta (Alex)

M: Middle of Delta (AL-Burullus)

E: East of Delta (Port Said)

## 2. Temperature and sea level rise

An IPCC-adopted track for greenhouse gas concentrations (not emissions) is known as a Representative Concentration Pathway (RCP). For the 2014 IPCC Fifth Assessment Report (AR5), four methodologies were employed for climate modeling and research. The pathways show various possible climatic futures, dependent on the amount of greenhouse gases (GHG) released in the upcoming years, all of which are thought to be possible. The RCPs, which were originally designated as RCP2.6, RCP4.5, RCP6, and RCP8.5, are titled for a potential range of radiative forcing levels in the year 2100 (2.6, 4.5, 6, and 8.5 W/m<sup>2</sup>, respectively) as shown in Table 2.

**Table 2:** Impact of temperature on SLR in different IPCC scenarios (RCP scenario) (Stocker, 2014)

Scenario	Description	Global warming ( °C) Mean and likely range		Global SLR (cm) Mean and likely range	
		2046-2065	2081-2100	2046-2065	2081-2100
RCP 8.5	Rising radiative forcing pathway leading to 8.5 W/m <sup>2</sup> ( ~1370 ppm CO <sub>2</sub> equivalent ) by 2100	2 (1.4-1.6)	3.7 (2.6-4.8)	30 (22-38)	63 (45-82)
	Stabilization without overshoot pathway 6.0 W/m <sup>2</sup> ( ~850 ppm	1.3	2.2	25	48



To describe and forecast how the groundwater system will behave, the MODFLOW code was created. In this model, the hydrodynamic modeling of groundwater flow in an anisotropic and heterogeneous medium under non-equilibrium conditions was carried out using finite-difference techniques. A simulation of changes in the concentration of miscible contaminants in groundwater can be made using MT3DMS with a choice of boundary conditions, external sources, and sinks. Considerations include advection, dispersion, and diffusion, as well as some basic chemical processes. Any Finite-Difference flow model that is block-centered, such as the modular Finite-Difference ground water flow model, can be used with MT3DMS. Transport of solutes is simulated using estimated hydraulic heads and other flow parameters from MODFLOW. The most recent version of the computer application SEWAT, called SEWAT2000, is used to simulate 3-D groundwater flow models across porous media with a changing density transient. SEWAT 2000 was produced by combining MT3DMS and MODFLOW 2000 into a single application. In addition to the integrated transport processes of MT3DMS and variable density flow, SEWAT 2000 include all of the processes that were present in the MODFLOW application.

## 5. parameters and methodology

### 5.1 Study area hydrology

Aquitard, Quaternary aquifer, and Aquiclude are the three primary hydrogeological components of the aquifer of the Nile Delta.

The top strata of the deposits in the delta, known as aquitard, were formed during the Holocene era (10,000 years). This formation is composed of semi-previous clay and sand. It is mostly heterogeneous and anisotropic. The Nile Delta aquifer's clay cover varies in thickness from 40 m in the north, middle, and western delta regions to 95 m in the eastern delta coast, disappearing near the aquifer's limits (Nofal et al., 2015).

The primary component of the aquifer is the quaternary aquifer. It is a large unit from the Pleistocene era that is made up primarily of gravel and coarse sand with some intercalation of clay lenses. The thickness of this strata increases northward. It varies from 150 m at El-Quanater El-Khairia in the south to more than 500 m next to Tanta before moving north till it reaches around 1000 m close to the Mediterranean Sea's shore (Bear et al., 1999).

### 5.2 Hydraulic input parameters

The most crucial parameter for hydraulics is hydraulic conductivity ( $k$ ), which is one of the parameters was taken as illustrated in (Figs. 4 and 5). Effective porosity ( $n_{eff}$ ), total porosity ( $n$ ), specific yield ( $Sy$ ), and specific storage ( $Ss$ ) also taken from previous studies. The aquifer is refilled by excess water from irrigation, which is thought to be the main contributor to aquifer recharge, as illustrated in (Figure 6). According to (Morsy, 2009) data from 2008, the total discharge amount was  $2.78 * 10^9 m^3/year$ . (Figure 7) shows the map of abstraction wells distribution in the study area (Abdelaty et al., 2014)

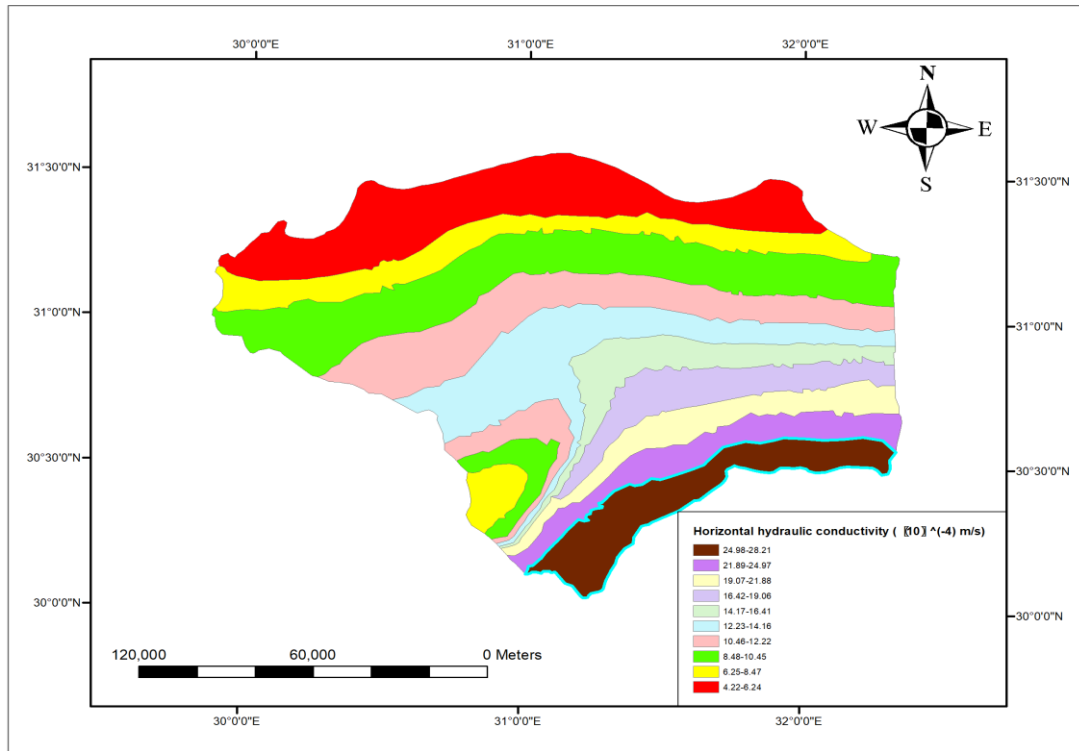


**Figure 4:** The calibrated horizontal hydraulic conductivity of the quaternary aquifer (Armanuos & Negm, 2018)

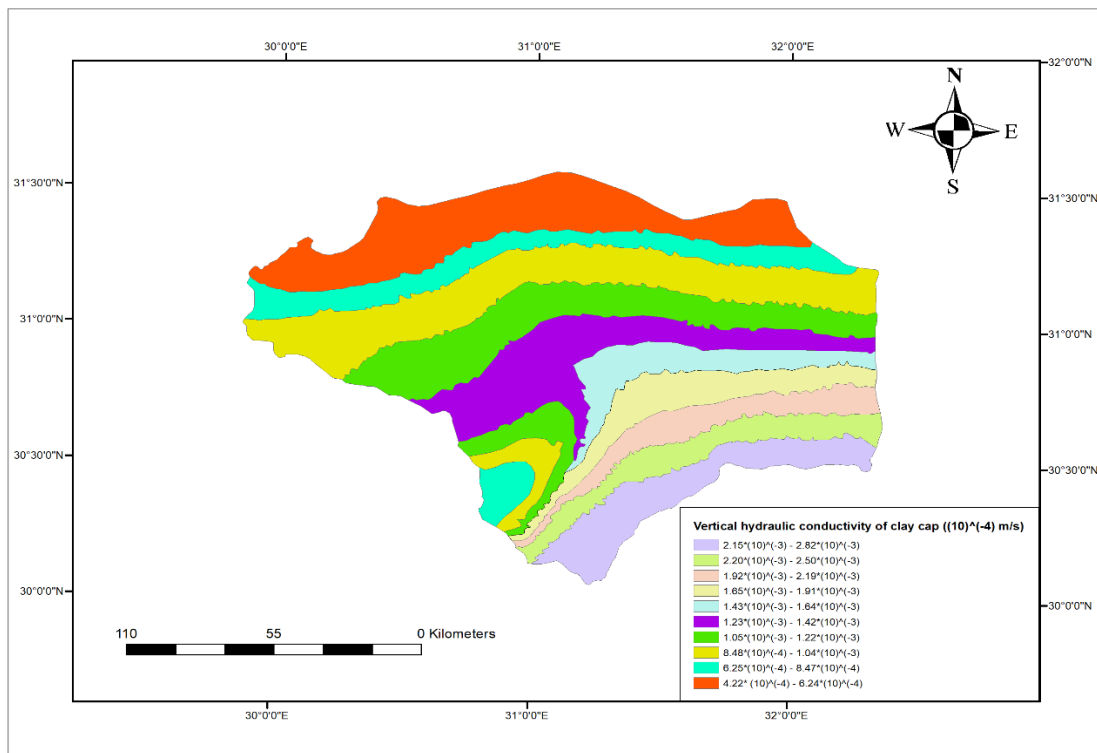


**Figure 5:** The calibrated vertical hydraulic conductivity of the first layer (Armanuos & Negm, 2018)

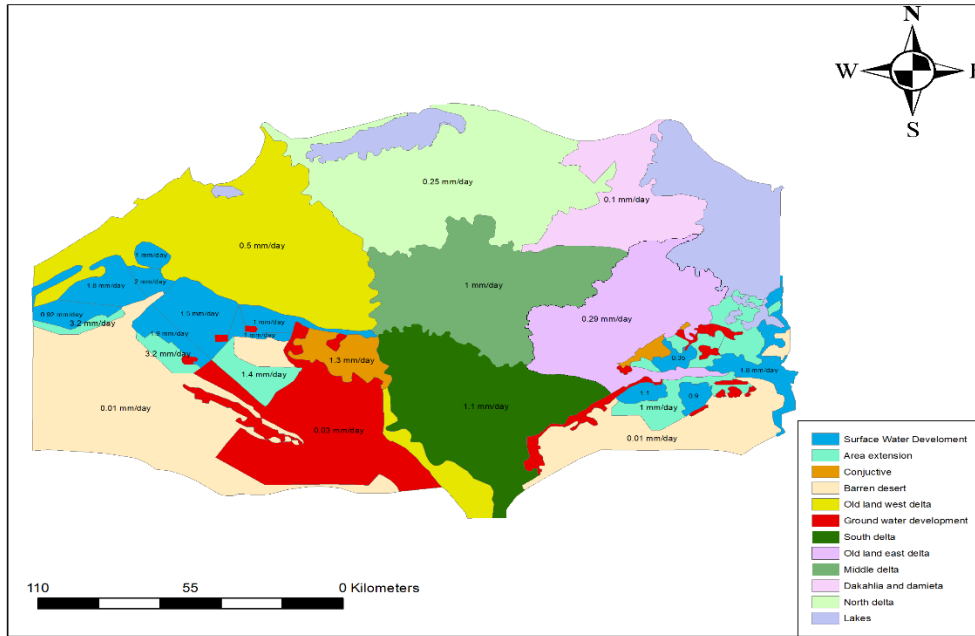


**Figure 6:** Distribution of drainage excess in the Nile Delta region in 2008 (Morsy, 2009)

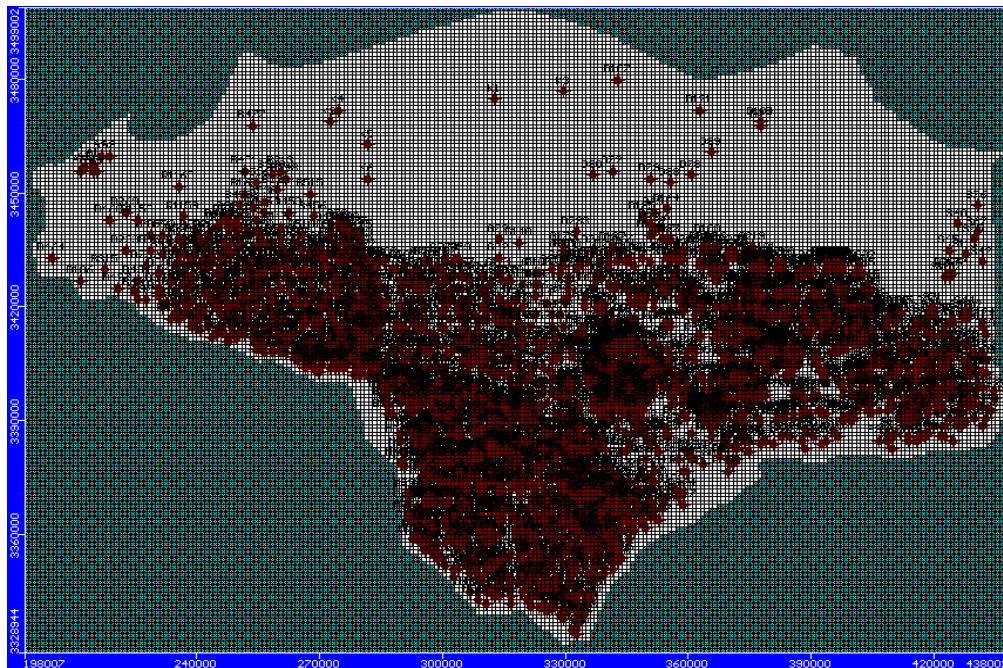


**Figure 7:** location map of abstraction wells (Abdelaty et al., 2014)

### 5.3 Model discretization

The simulated model's research area is approximately  $40,800 \text{ km}^2$  and extends over a length of 240 km in an east-west direction and 170 km in a north-south direction. All active and inactive cells are separated into 240 columns and 170 rows in the model. The cell dimensions is  $1000 \text{ m} * 1000 \text{ m}$ . (Figure8) shows the aquifer's horizontal cross section. The aquifer's vertical thickness varies from 200 m in the south near Cairo to 1000 m in the north near the Mediterranean sea. Eleven layers make up the vertical thickness; the first layer, which has an average depth of 50 metres, represents the aquifer's clay cover, while layers two through eleven constitute the quaternary aquifer. (Figure9-a) illustrates the vertical cross section from north to south in Y direction. (Figure9-b) reveals the vertical from east to west cross section in X direction.

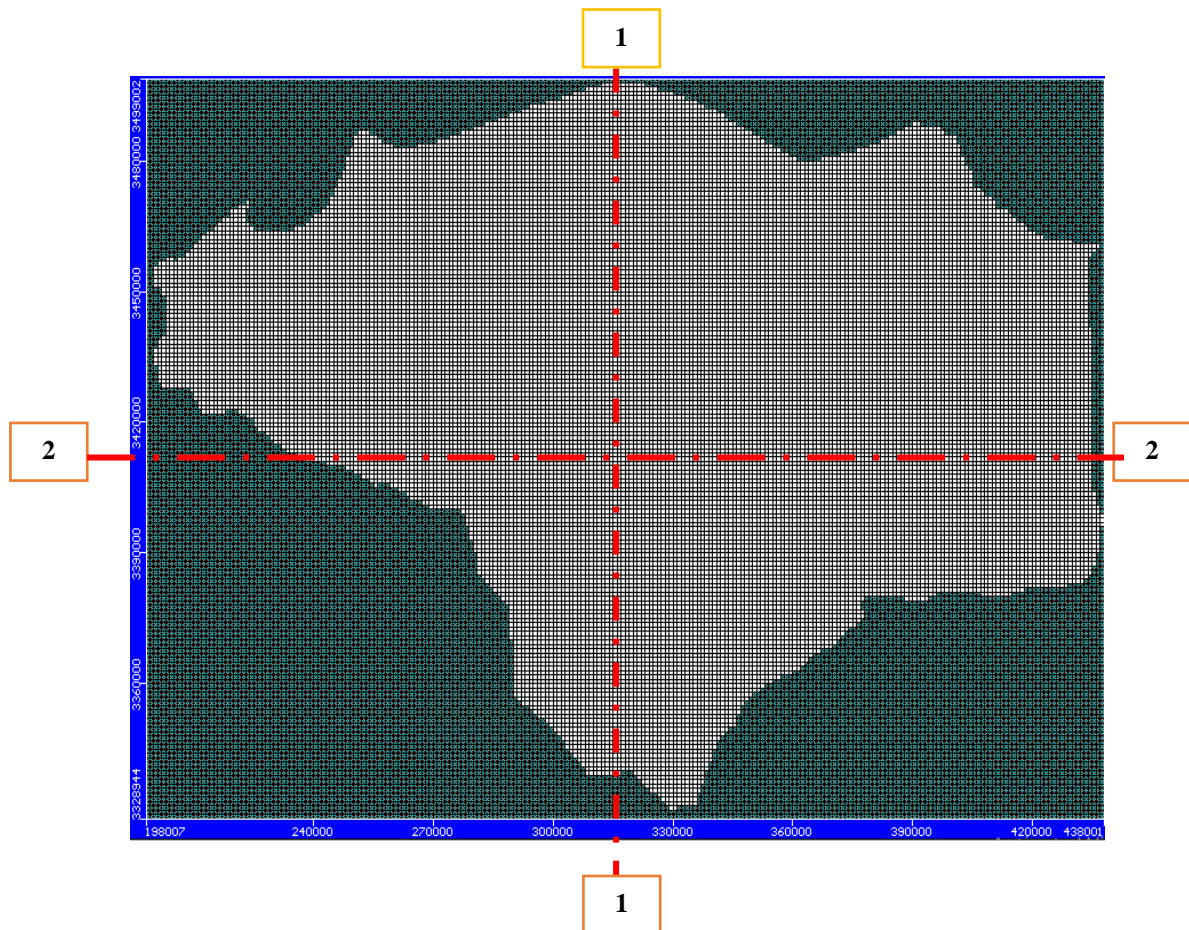


**Figure 8:** Discretization of the aquifer of Nile Delta

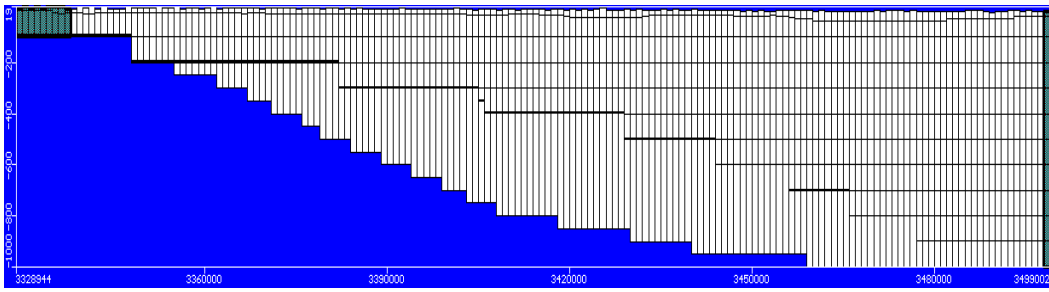


Figure 9-a: The Nile Delta aquifer model's Vertical cross section Sec (1-1)

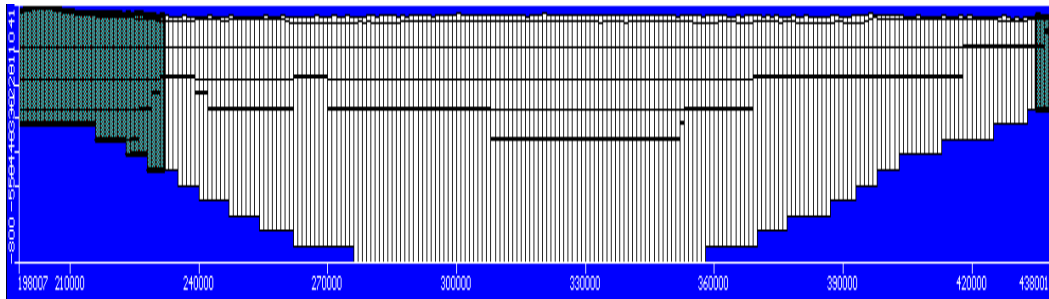


Figure 9-b: The Nile Delta aquifer model's Vertical cross section Sec (2-2)

5.4 Boundary and initial conditions

The coastline border of the Mediterranean Sea is represented by a constant head, which is assumed to be zero, and a constant concentration, which is assumed to be 40,000 mg/l. The constant head, which is taken to be 16.96 m near Cairo, is used to denote the southern border, and it refers to the presence of the Delta Barrage. Constant concentration, which equals 35,000 mg/l, represents the eastern boundary along the Suez Canal and the Red Sea. Ismailia canal at the south east border (starting head=18.5m, Ending head=7.6m), Nubaria canal and Rayah Nassri at the west boundary (starting head=18.3m, Ending head =2.92m) from natural boundary which is controlled. (Figure 10) illustrates the boundary conditions in Nile Delta.

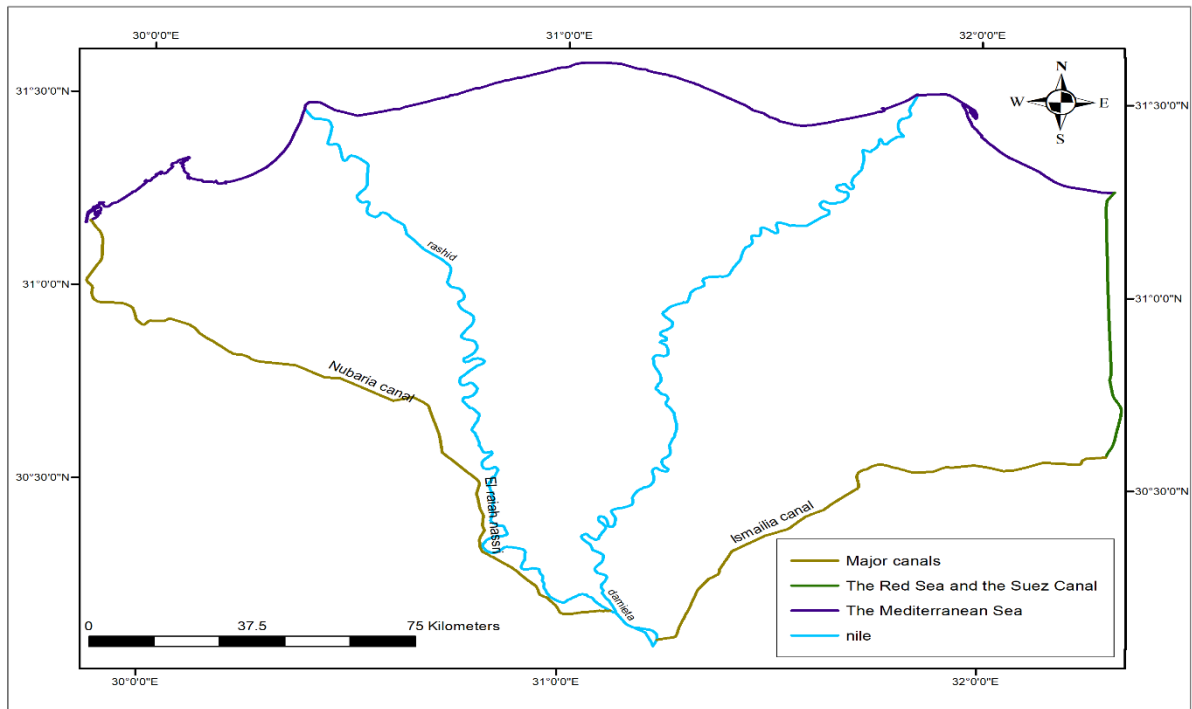
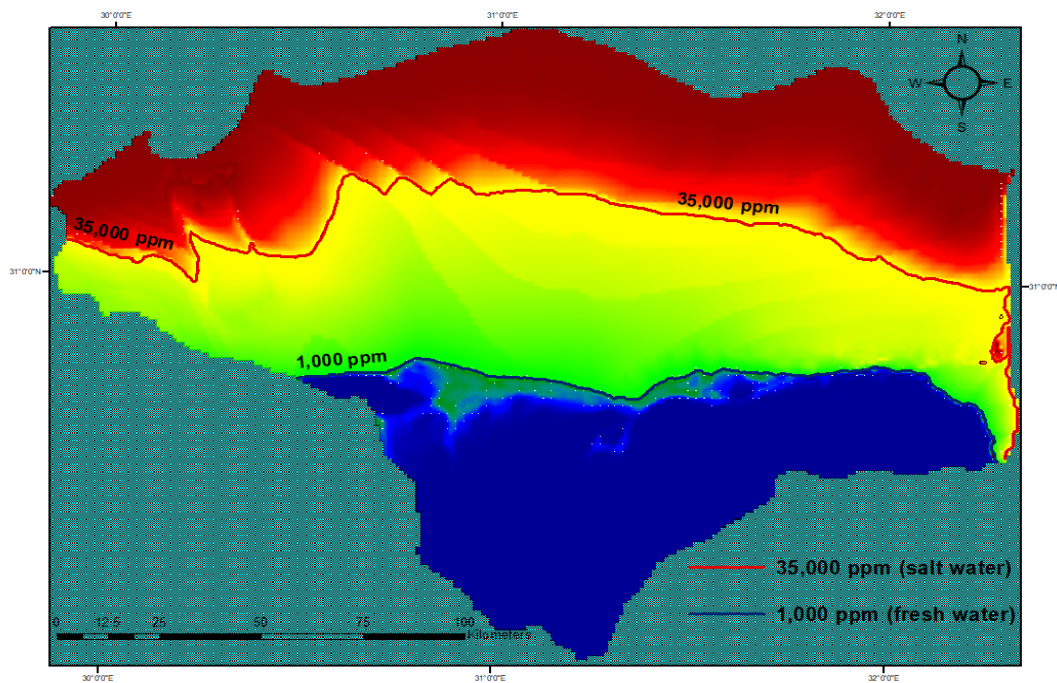


Figure 10: Nile Delta region boundary conditions (Sefelnasr & Sherif, 2014)

### 5.5 Simulation of base case and calibration of the groundwater salinity model

The model was used using the 2008 data that was available, and this case was treated as the base case. Salt water intrusion distributions are the important output of transport model. (Figure 11), with an average depth of 1000 m in the north and 200 m in the south, displays the distribution of TDS at layer 11 (at the base of the aquifer). In the Nile delta, three cross sections are taken: cross section 1 towards the west, cross section 2 at the middle, and cross section 3 at the east. The equiconcentration line 35,000 ppm, which expresses salt water, travelled inland to a distance of 40 km from the shoreline line at cross section 1, The equiconcentration line 1,000 ppm which distinguishes fresh water from salt water, travelled farther inland to a distance of 67 km (Figure 12-a). The equiconcentration line 35,000 ppm moved inland to a distance of 43 km from the shore at cross section 2, the equiconcentration line 1,000 ppm advanced inland to a distance of 93 km (Figure 12-b). The equiconcentration line 35,000 ppm progressed inland to a distance of 50 km from the shoreline line at cross section 3, The equiconcentration line 1,000 ppm travelled 81 kilometres inland (Figure 12-c).



**Figure 11:** TDS Horizontal Distribution at the base of Nile Delta Aquifer

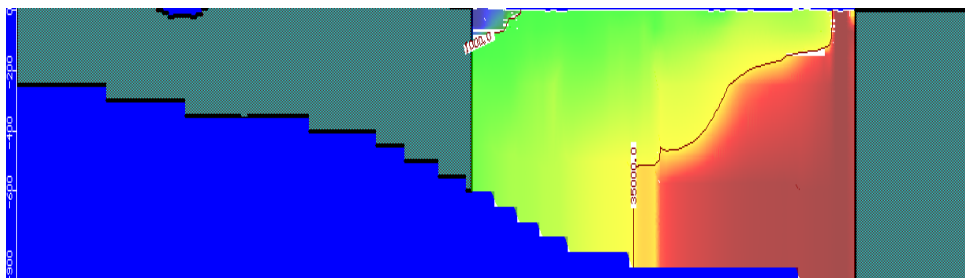


**Figure 12-a:** Nile Delta's aquifer's vertical salt concentration distribution for the basic case at cross sections 1 (west)

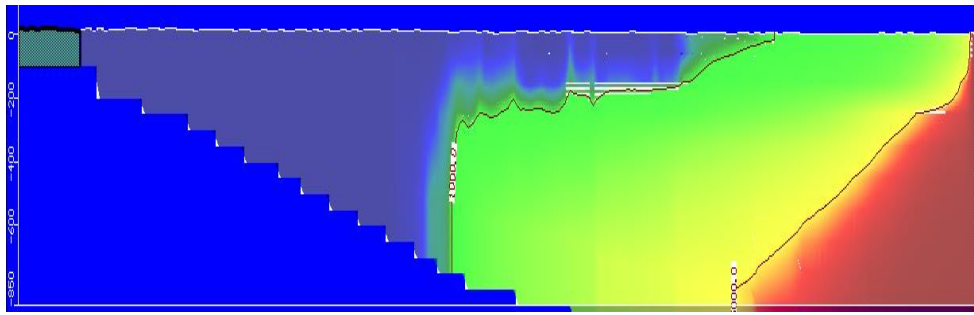


**Figure 12-b:** Nile Delta's aquifer's vertical salt concentration distribution for the basic case at cross sections 2 (Middle)

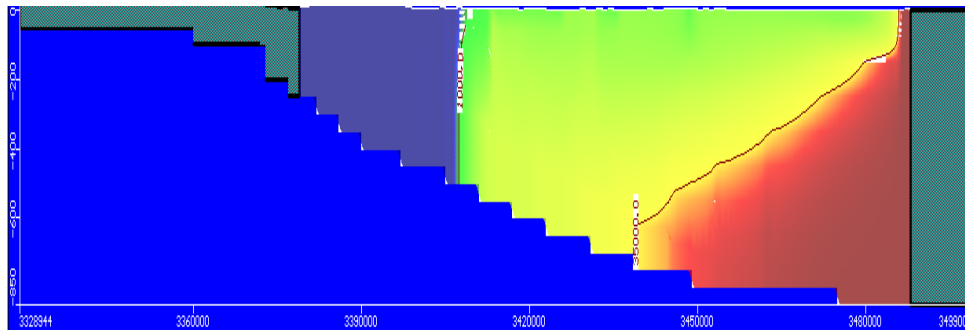


**Figure 12-c:** Nile Delta's aquifer's vertical salt concentration distribution for the basic case at cross sections 3 (East)

Between the salinity of simulated ground water and that of recently completed investigations, a calibration process was made. In the base situation, the calibration is based on the advancement of the equiconcentration lines 35,000 ppm and 1,000 ppm inland. The calibration revealed good agreement between the results of recent research and simulations as shown in Table 3.

**Table 3:** Comparison of the most recent studies and the present research.

Study		Current study	(Sefelnasr & Sherif, 2014)	(Abdelaty et al., 2014)	(Elshinnawy et al., 2015)	(Armanuos & Negm, 2018)
Position	Line					
West	Equi-line 35,000 ppm	40 km	37 km	48 km	23 km	40 km
	Equi-line 1,000 ppm	67 km	66 km	72.5 km	53 km	66 km
Middle	Equi-line 35,000 ppm	43 km	43 km	63.75 km	43.5 km	56 km
	Equi-line 1,000 ppm	93 km	75 km	93.75 km	68 km	105 km
East	Equi-line 35,000 ppm	50 km	50 km	76.25 km	33.5 km	75 km
	Equi-line 1,000 ppm	81 km	86 km	90.75 km	78 km	100 km

## 6. Results and discussion

An investigation of the creep of saltwater in the aquifer of Nile Delta throughout the previous 60 years is conducted. The equiconcentration line 1,000 ppm of this study was compared with the equiconcentration line 1,000 ppm of the following years 1960, 1980, and 1992 which were taken from (Morsy, 2009). The Results showed that the equiconcentration line 1,000 migrated inland a distance of 55 km, 59 km, 44 km, and 67 km from the shore line at west, 72.5km, 70 km, 65 km, and 93 km at middle, 83.5 km, 90 km, 93 km, and 81 km

at east for the years 1960,1980,1992, and 2022 respectively. It is clear that the creep of salt water increases at west and middle, but decreases at east of Nile delta as shown in (Figure 13).The location of the new shore line due to 0.25 m and 0.5 m of sea level rise is determined based on approximation dependent on the previous studies, because there is a lack of information regarding the topography of the research region and it requires high accuracy of Digital Elevation Model (DEM). The most recent studies are analyzed for logical results. (Armanuos et al., 2022) used (MODFLOW + SEWAT) and found that for a **0.25** m rise in sea level, equiconcentration line 35,000 ppm advanced inland 44.19 km in the west, 58.35 km in the middle, and 79.11 km in the east, and equiconcentration line 1,000 ppm advanced inland 67.90 km in the west, 106.9 km in the middle, and 105.5 km in east. For a **0.5** m rise in sea level, it is predicted that equiconcentration line 35,000 ppm intruded inland at 44.51 west, 59.09 middle, and 81.10 east, and equiconcentration line 1,000 ppm intruded inland at 68 west, 107.4 middle, and 105.56 east. These data were analyzed through (MODFLOW+SEAWAT) and the results were exported to ARCGIS to determine the new shoreline's location, as illustrated in (Figs 14-a, 14-b and 14-c).

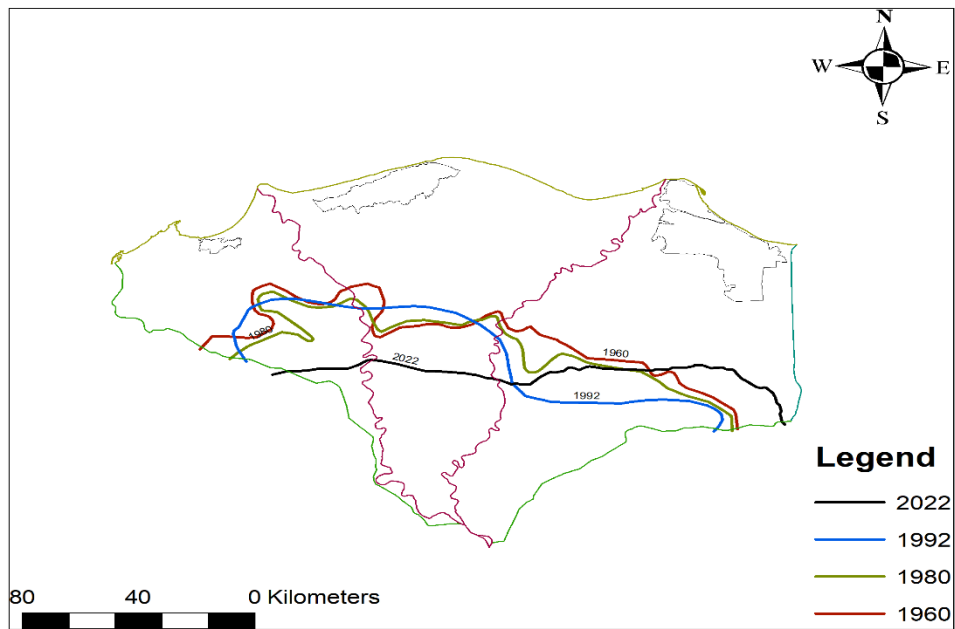


Figure 13: TDS (salinity) in groundwater in 1960, 1980, 1992, and current study (2022)

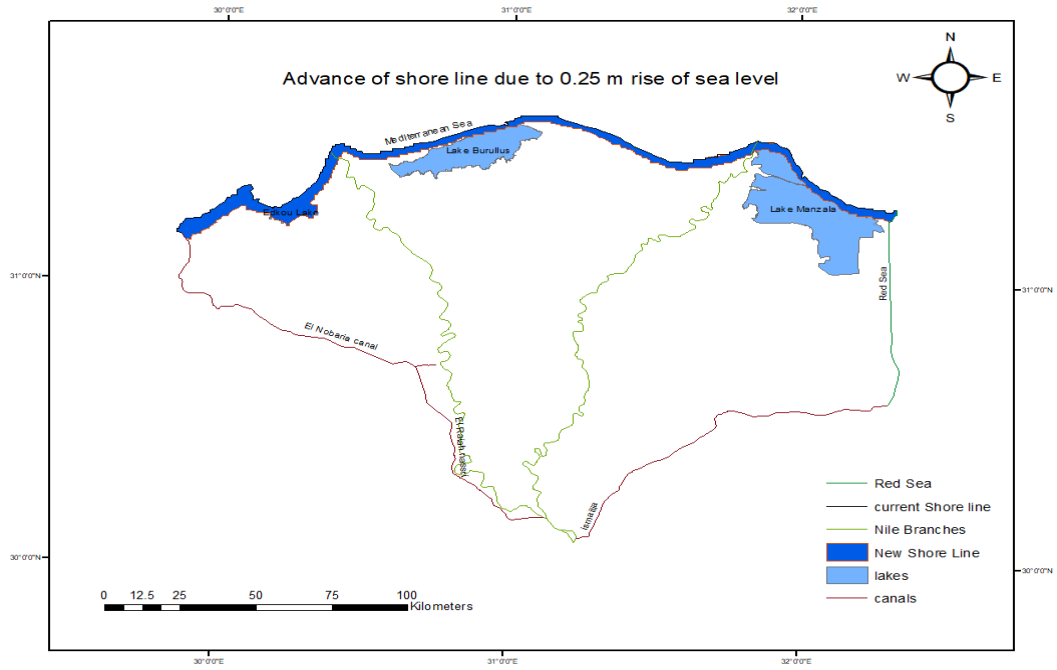


Figure 14-a: position of the shoreline as a result of the 0.25 m sea level rise

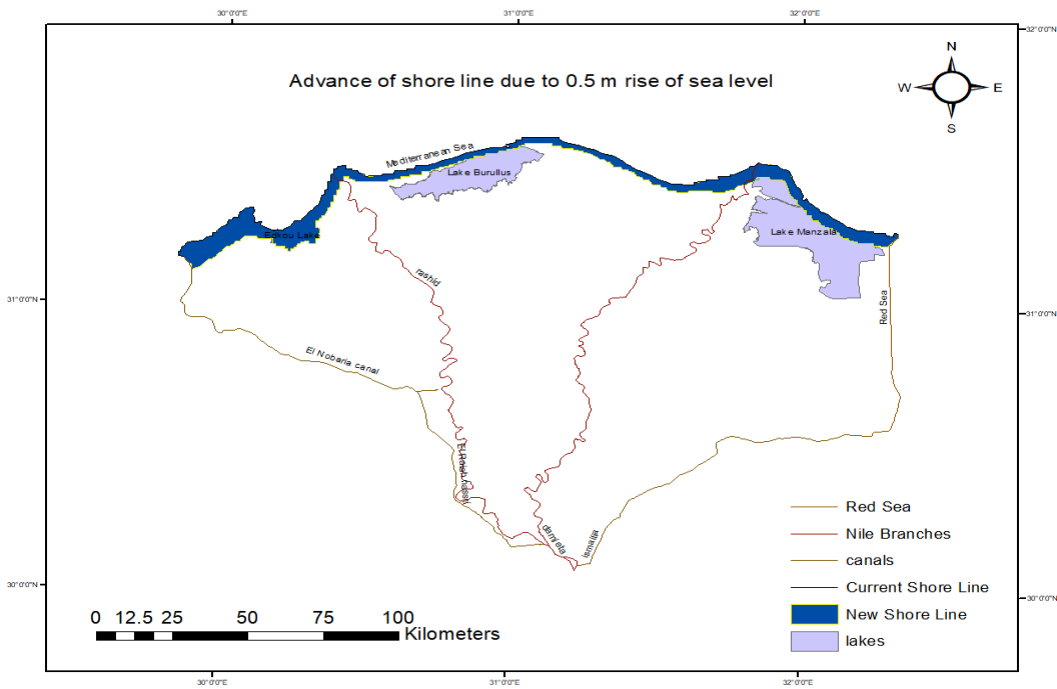


Figure 14-b: position of the shoreline as a result of the 0.5 m sea level rise

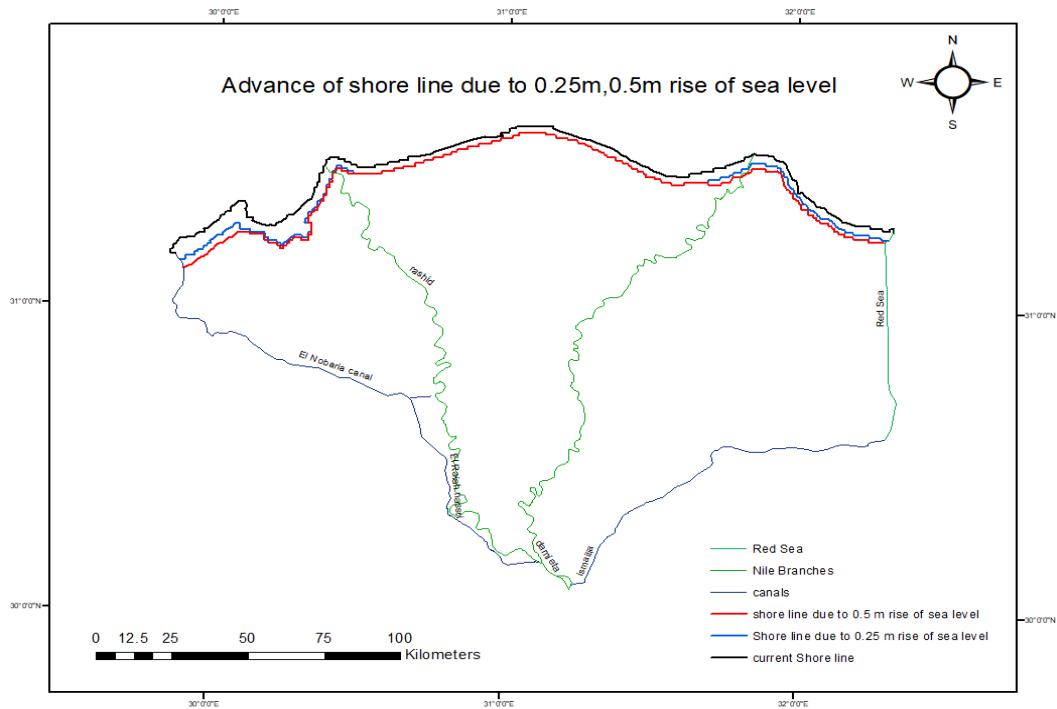


Figure 14-c: position of the shoreline as a result of the 0.25 m, 0.5 m sea level rise

## 7. Conclusion

The main objectives of this study are to investigate seawater intrusion in Nile Delta aquifer and determine the new position of shore line due 0.25 m and 0.5 m rise of sea level in Nile Delta. For the purpose of completing the requirements of this study, numerous activities have been established. **ARC.GIS**, visual **MODFLOW** and **SEAWAT** were used. The results of the simulation of salinity for base case showed that a significant portion of the Nile delta aquifer is polluted by saline water in base case without any external factors. The results of base case for equiconcentration line 35,000 ppm and 1,000 ppm were calibrated, comparing it with the results of most recent studies. The calibration showed a good relevant between simulated and results of recent studies. An investigation was applied to investigate the creep of salt water during the last 60 years and showed that, the creep of saltwater occurs at a large scale in west and middle counter to east where the creep is more slower in compared with years 1960, 1980 and 1992. The position of equiconcentration line 35,000 ppm and equiconcentration line 1,000 ppm of the most recent data for 0.25m and 0.5m sea level rise were analyzed , using (MODFLOW+SEWAT). Using ARC GIS, three maps were obtained, one of which represents the location of the new shore line as a result of the sea level rise of 0.25 meters, and the other represents the location of the new shore line as a result of the sea level rise of 0.5 meters, and the third combines the location of the two previous lines together.

## 8. References

- Abd-Elhamid, H. F. (2010). A simulation-optimization model to study the control of seawater intrusion in coastal aquifers.
- Abdelaty, I. M., Abd-Elhamid, H. F., Fahmy, M. R., & Abdelaal, G. M. (2014). Investigation of some potential parameters and its impacts on saltwater intrusion in Nile Delta aquifer. *JES. Journal of Engineering Sciences*, 42(4), 931-955.
- Agrawala, S., Moehner, A., El Raey, M., Conway, D., Van Aalst, M., Hagenstad, M., & Smith, J. (2004). Development and climate change in Egypt: focus on coastal resources and the Nile. *Organisation for Economic Co-operation and Development*, 1, 1-68.
- Armanuos, A. M., Eldin Ibrahim, M. G., Negm, A., Takemura, J., Yoshimura, C., & Mahmod, W. E. (2022). Investigation of Seawater Intrusion in the Nile Delta Aquifer, Egypt. *Journal of Engineering Research*, 6(1), 10-28.
- Armanuos, A. M., Ibrahim, M. G., Mahmod, W. E., Negm, A., Yoshimura, C., Takemura, J., & Zidan, B. A. (2017). Evaluation of the potential impact of Grand Ethiopian Renaissance Dam and pumping scenarios on groundwater level in the Nile Delta aquifer. *Water Science and Technology: Water Supply*, 17(5), 1356-1367.

- Armanuos, A. M., & Negm, A. (2018). Integrated groundwater modeling for simulation of saltwater intrusion in the Nile Delta aquifer, Egypt. In *Groundwater in the Nile Delta* (pp. 489-544). Springer.
- Bear, J., Cheng, A. H.-D., Sorek, S., Ouazar, D., & Herrera, I. (1999). *Seawater intrusion in coastal aquifers: concepts, methods and practices* (Vol. 14). Springer Science & Business Media.
- CORI. (2008). *Coastal Vulnerability to Climate Changes and Adaptation Assessment for Coastal Zones of Egypt, Final Report*, Wikipedia, URL: <http://en.wikipedia.org/wiki/NileDelta>.
- El-Raey, M. (1994). Vulnerability Assessment of the Coastal Zone of Egypt to the Impacts of Sea Level Rise. Phase III, US Country Study Program.
- Elshinnawy, H., Zeidan, B., & Ghoraba, S. (2015). Impact of hydraulic conductivity uniformity on seawater intrusion in the Nile Delta aquifer, Egypt. In.
- IPCC. (2001). *Climate Change 2001: Impacts, Adaptations, and Vulnerability: contribution of working group II to the third assessment report of the Intergovernmental Panel on Climate Change*. Mc Carthy, J. J., Canziani, O. F., Leary, N. A., Dokken, D. J. and White, K. S. Cambridge University Press, Cambridge, UK and New York, NY, USA
- Ismail, I. A.-E. M. (2014). *Numerical and Experimental Study for Simulating Climatic Changes Effects on Nile Delta Aquifer* Faculty of Engineering, Zagazig University].
- Kashef, A. A. I. (1983). Salt-Water Intrusion in the Nile Delta. *Groundwater*, 21(2), 160-167.
- Morsy, W. S. (2009). *Environmental Management to Groundwater Resources for Nile Delta Region* [phD thesis, Faculty of Engineering, Cairo University].
- Nofal, E., Amer, M., El-Didy, S., & Fekry, A. (2015). Sea water intrusion in Nile Delta in perspective of new configuration of the aquifer heterogeneity using the recent stratigraphy data. *J Am Sci*, 11(6), 281-292.
- RIGW. (1992). Hydrogeological map of Egypt, Nile Delta Scale 1: 50000000. NWRC, Cairo, Egypt.
- RIGW. (2002). *Nile Delta groundwater modeling report. Research Institute for Groundwater*.
- Sefelnasr, A., & Sherif, M. (2014). Impacts of seawater rise on seawater intrusion in the Nile Delta aquifer, Egypt. *Groundwater*, 52(2), 264-276.
- SNC. (2010). Egypt's Second National Communication, Egyptian Environmental Affairs Agency (EEAA-May 2010), under the United Nations Framework Convention on Climate Change on Climate Change.
- Stocker, T. F., Qin, D., Plattner, G. K., Tignor, M. M., Allen, S. K., Boschung, J., ... & Midgley, P. M. (2014). *Climate Change 2013: The physical science basis. contribution of working group I to the fifth assessment report of IPCC the intergovernmental panel on climate change*.